The Astrophysical Journal Letters, 783:L12 (5pp), 2014 March 1 doi:10.1088/2041-8205/783/1/L12

CHARACTERIZING FAINT GALAXIES IN THE REIONIZATION EPOCH: LBT CONFIRMS TWO $L < 0.2\,L^{\star}$ SOURCES AT $z = 6.4$ BEHIND THE CLASH/FRONTIER FIELDS CLUSTER MACS0717.5+3745*

E. Vanzella[1], A. Fontana[2], A. Zitrin[3,12], D. Coe[4], L. Bradley[4], M. Postman[4], A. Grazian[2], M. Castellano[2], L. Pentericci[2], M. Giavalisco[5], P. Rosati[6], M. Nonino[7], R. Smit[9], I. Balestra[8], R. Bouwens[9], S. Cristiani[7,8], E. Giallongo[2], W. Zheng[10], L. Infante[11], F. Cusano[1], and R. Speziali[2]
[1] INAF–Bologna Astronomical Observatory, via Ranzani 1, I-40127 Bologna, Italy
[2] INAF–Rome Astronomical Observatory, Via Frascati 33, I-00040 Monteporzio Roma, Italy
[3] Cahill Center for Astronomy and Astrophysics, California Institute of Technology, MS 249-17, Pasadena, CA 91125, USA
[4] STScI, 3700 San Martin Drive, Baltimore, MD 21218, USA
[5] Department of Astronomy, University of Massachusetts, Amherst, MA 01003, USA
[6] Dipartimento di Fisica e Scienze della Terra, Università di Ferrara, via Saragat 1, I-44122 Ferrara, Italy
[7] INAF, Astronomical Observatory of Trieste, via G.B. Tiepolo 11, I-34143 Trieste, Italy
[8] INFN, National Institute of Nuclear Physics, via Valerio 2, I-34127 Trieste, Italy
[9] Leiden Observatory, Leiden University, P.O. Box 9513, 2300 RA Leiden, The Netherlands
[10] Department of Physics and Astronomy, The Johns Hopkins University, 3400 North Charles Street, Baltimore, MD 21218, USA
[11] Institute of Astrophysics, Pontificia Universidad Catolica de Chile, V. Mackenna 4860, 22 Santiago, Chile
Received 2013 December 23; accepted 2014 January 27; published 2014 February 14

ABSTRACT

We report the LBT/MODS1 spectroscopic confirmation of two images of faint Lyα emitters at $z = 6.4$ behind the Frontier Fields galaxy cluster MACSJ0717.5+3745. A wide range of lens models suggests that the two images are highly magnified, with a strong lower limit of $\mu > 5$. These are the faintest $z > 6$ candidates spectroscopically confirmed to date. These may also be multiple images of the same $z = 6.4$ source as supported by their similar intrinsic properties, but the lens models are inconclusive regarding this interpretation. To be cautious, we derive the physical properties of each image individually. Thanks to the high magnification, the observed near-infrared (restframe ultraviolet) part of the spectral energy distributions and Lyα lines are well detected with S/N(m_{1500}) $\gtrsim$ 10 and S/N(Lyα) $\simeq$ 10–15. Adopting $\mu > 5$, the absolute magnitudes, M_{1500}, and Lyα fluxes are fainter than -18.7 and 2.8×10^{-18} erg s^{-1} cm^{-2}, respectively. We find a very steep ultraviolet spectral slope $\beta = -3.0 \pm 0.5$ ($F_{\lambda} = \lambda^{\beta}$), implying that these are very young, dust-free, and low metallicity objects, made of standard stellar populations or even extremely metal poor stars (age $\lesssim$ 30 Myr, $E(B-V) = 0$ and metallicity 0.0–0.2 $Z/Z_{\odot}$). The objects are compact (<1 kpc^2) and with a stellar mass $M_{\star} < 10^8\,M_{\odot}$. The very steep β, the presence of the Lyα line, and the intrinsic FWHM (<300 km s^{-1}) of these newborn objects do not exclude a possible leakage of ionizing radiation. We discuss the possibility that such faint galaxies may resemble those responsible for cosmic reionization.

Key words: cosmology: observations – dark ages, reionization, first stars – galaxies: formation

Online-only material: color figures

1. INTRODUCTION

The investigation of the distant universe and the processes that led to the reionization of the intergalactic medium (IGM) are among the major goals of observational cosmology (Robertson et al. 2010). While there are tens (a few) of spectroscopic confirmations of galaxies at redshift 6(7) (e.g., Vanzella et al. 2009, 2011), accessing the faint-luminosity regime down to $\lesssim 0.2\,L^{\star}$ remains challenging even with the 8–10 m class telescopes, especially for $z > 6$. Before the advent of next generation observatories like *James Webb Space Telescope* (*JWST*) and the extremely large telescopes, the only viable way to pursue extremely faint distant objects, and investigate the nature of their stellar populations (even PopIII), is to exploit strong lensing magnification (e.g., Zackrisson et al. 2012, 2013). To this aim, Bradley et al. (2013, B13 hereafter) selected magnified candidate galaxies at redshifts 68, fully exploiting the 16-band photometry of the CLASH survey (Postman et al. 2012) and found agreement down to ~27 mag with the UV luminosity functions of blank fields. After the completion of the CLASH program, the investigation of the high-z universe is now continuing with the ultradeep *Hubble Space Telescope* (*HST*) Frontier Fields campaign (FF hereafter), which includes four CLASH galaxy clusters.[13]

Accessing the faint luminosity regime ($L \lesssim 0.2\,L^{\star}$) at $z > 6$ is crucial in the context of cosmic reionization (e.g., Fontanot et al. 2013): faint galaxies dominate the global ultraviolet luminosity density (Bouwens et al. 2007) and possibly have an escape fraction of ionizing radiation larger than the brighter counterparts (e.g., Ferrara & Loeb 2013; Yajima et al. 2011).

Here we report on the LBT/MODS1 spectroscopic confirmation of two faint $z = 6.4$ sources, which are significantly magnified by the FF galaxy cluster MACSJ0717.5+3745 (Ebeling et al. 2007), study their physical properties, and discuss the contributions of such objects to the reionization of the IGM.

Throughout this Letter, a concordance ΛCDM cosmology with $\Omega_m = 0.3$, $\Omega_{\Lambda} = 0.7$ and $H_0 = 70$ km s^{-1} Mpc^{-1} is adopted, and magnitudes are in AB scale.

* The Large Binocular Telescope (LBT) is an international collaboration among institutions in the United States, Italy, and Germany. LBT Corporation partners are: The University of Arizona on behalf of the Arizona university system; Istituto Nazionale di Astrofisica, Italy; LBT Beteiligungsgesellschaft, Germany, representing the Max-Planck Society, the Astrophysical Institute Potsdam, and Heidelberg University; The Ohio State University; and The Research Corporation, on behalf of The University of Notre Dame, University of Minnesota, and University of Virginia.
[12] Hubble Fellow.
[13] http://www.stsci.edu/hst/campaigns/frontier-fields/

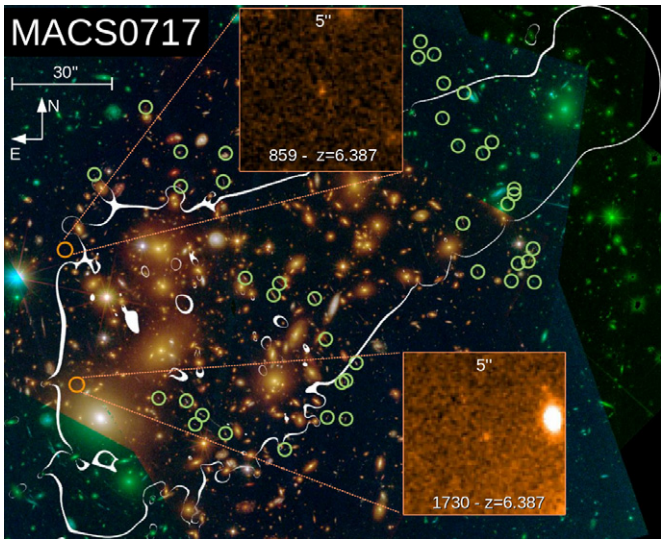

Figure 1. Sixteen-band CLASH RGB false-color image of MACSJ0717.5+3745, with the two $z = 6.4$ spectroscopically confirmed images marked with red circles (the insets show the J125 zoom). The critical curves ($\mu > 100$ here) for a source at $z_s = 6.4$ from the revised Zitrin et al. model are overlaid in white. The green circles mark the multiple images used as constraints (see Zitrin et al. 2009; Limousin et al. 2012; Medezinski et al. 2013). As can be seen, the two $z = 6.4$ objects lie (1) close to the critical curves, and (2) in regions in which there are hardly other multiple images known, so that the exact position of the critical curves is not perfectly constrained. The proximity to the critical curves results in very high magnifications, of the order of a few to a few dozen, and correspondingly, large errors on these estimates. Still, all probed models (see Section 2.1) yield $\mu > 5$ for both images, which we have adopted throughout this work as our lower limit, for conservative results.

(A color version of this figure is available in the online journal.)

1.1. Target Selection and Magnification

B13 selected 15 magnified $z \simeq 6$ galaxy candidates behind the FF galaxy cluster MACSJ0717.5+3745 by using their drop-out features and corresponding photometric redshift estimate. We report here the spectroscopic observations of two candidates from their sample, macs0717_0859 and macs0717_1730 (859 and 1730 for short, hereafter), with photometric redshifts of 6.1 ± 0.2 and $6.0^{+0.2}_{-0.3}$, respectively. The magnifications reported in B13 were $\mu = 15.6$ (859) and $\mu > 100$ (1730) (i.e., the latter is unconstrained since the object is too close to the critical curves). The magnification estimates were based on the revised lens model by Zitrin et al. (2009; see also Medezinski et al. 2013) who first performed the strong-lensing analysis for this cluster, uncovering the largest magnifying lens known to date (see Figure 1). Here we have also estimated the magnifications from several other lens models made for the Frontier Fields program (including a refurbished version of the Zitrin et al. model used in B13) by running the Magnification Calculator available online.[14] The estimate from different groups, methods, and assumptions span the range between 5 and 70, with some solutions even higher than 100 within the 68% confidence interval. The medians among the different models are: $\mu = 17.4^{+25}_{-13}(^{+50}_{-12})$ for 1730 and $\mu = 6.9^{+1}_{-1}(^{+30}_{-2})$ for 859, where statistical and systematic errors (in parentheses) are quoted. The models for this lens are still not fully constrained in the regions where the two $z = 6.4$ are detected, both due to proximity to the critical curves, and lack of multiple-image constraints nearby. We also acknowledge the possibility that the two sources presented here are actually counter-images of a single background galaxy, as some of the models provided by the different groups predict counter-images within a few to a dozen arcseconds from the location of the other $z = 6.4$ object. We did not, however, detect any additional counter-images where the models predict them (although possibly due to lesser magnification where other images are predicted).

As not all models predict counter-images, and predicted counter-images were not identified in the data, it cannot be unambiguously determined if indeed the two objects are images of the same source. What is relevant here, though, is the agreement among the different models that the sources are strongly magnified ($\mu > 5$), and the single or double nature does not alter our findings on the derived physical properties. In the following, to be most conservative, we derive rest-frame quantities by adopting $\mu = 5$ for both sources and express the results in terms of $\mu_5 = \mu/5$.

2. DATA AND SAMPLE SELECTION

2.1. Spectroscopic Observations with LBT/MODS1

The spectroscopic observations have been performed in dual mode with the MODS1 instrument at the Large Binocular Telescope (LBT), which exploits the two red (5800–10300 Å) and blue (3200–6000 Å) channels, yielding a total spectra coverage from 3200 to ∼10300 Å on source. The red G670L and blue G400L grisms with a slit width of 1″ were adopted, providing a spectral resolution of $R \simeq 1500$ for both. Science frames of 1200 s have been acquired with a dithering pattern of 1.″5 shift along the slit for a total integration time of 16,800 s for 859, and 11,200 s for 1730. The average seeing conditions were ≃1.″0. Data reduction has been performed with the MODS1 spectroscopic reduction pipeline based on VIPGI tasks (Scodeggio et al. 2005).[15] In the two slits located on 859 and 1730, two emission lines are clearly detected at 8980 Å and 8981 Å, respectively, with observed fluxes of 1.4×10^{-17} erg s^{-1} cm^{-2} (with S/N = 15) and $\simeq 1.0 \times 10^{-17}$ erg s^{-1} cm^{-2} (with S/N = 9), respectively (see Figures 2 and 3).

3. RESULTS

1. *Nature of the lines.* The large spectral coverage (3200–10300 Å) allows us to exclude low redshift solutions like Hα at $z = 0.37$ or [O III] λ5007 at $z = 0.79$, which would be in contrast with the single line detection. The only possible degeneracy is between [O II] λ3727 and Lyα. However, [O III] λ3727 can be reliably excluded because of the following reasons: (1) the doublet [O II] λ3726–3729 is resolved in the present observations (see example in Figure 2, panel C) and (2) the observed equivalent width (see below) of the lines is not compatible with the typical values observed at $z < 1.5$, i.e., they are too large (e.g., Vanzella et al. 2009 and their Figure 12). Moreover, source 859 shows an asymmetric line profile toward the red wavelengths (Figure 3), which is typical of this transition at high redshift. The spectrum of 1730 is slightly shallower (11,200 s) and noisier than 859 (close to the edge of the slit), and prevents us from detecting the asymmetric shape, but the line width and the equivalent width are not consistent with the [O II] λ3727 doublet.

[14] http://archive.stsci.edu/prepds/frontier/lensmodels/

[15] http://lbt-spectro.iasf-milano.inaf.it/pipelinesInfo/

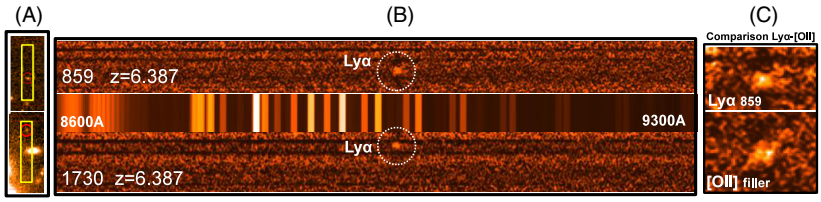

Figure 2. Panel (A): the position of targets 859 (top) and 1730 (bottom) in the MODS1 slits over the J125 band are shown. Panel (B): the two dimensional spectra with the Lyα lines (marked with dotted circles) and the sky spectrum are shown. Panel (C): The Lyα line of 859 compared with a low-z [O II] 3727 doublet (tilted) identified in the same mask (filler object) is shown.

(A color version of this figure is available in the online journal.)

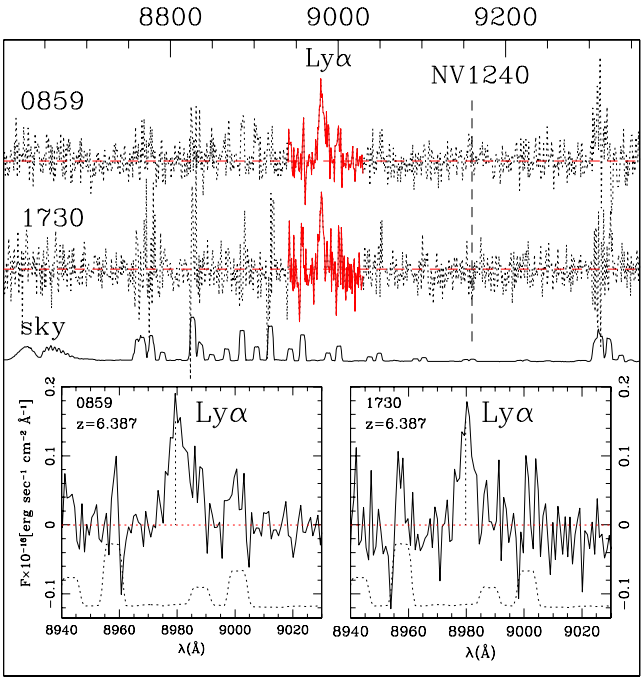

Figure 3. One-dimensional spectra of 859 and 1730 (top dotted). The parts of the spectra highlighted in red are zoomed in the bottom panels with the sky spectrum (dotted). The position of the N v λ1240 line is also shown with a vertical dashed line.

(A color version of this figure is available in the online journal.)

Therefore, we conclude that the two emission lines are Lyα at the same redshift 6.387 ± 0.002. The striking concordance of the two redshifts may add support to the hypothesis that these two objects are multiple images of the same background source. If confirmed, this could provide further constraints to the lens model and therefore deserves future investigation and lens remodeling, which is out of the scope of the present work. In the following we assume that these are two individual objects and look at the properties of each of them separately.

2. *Rest frame UV continuum luminosity at 1500 Å.* As mentioned above the wide spread of the magnifications allows us to identify an interval of possible luminosities. Given the observed Y105 magnitudes ($\simeq$1500 Å) of 26.42 ± 0.11 for 859 and 26.34 ± 0.16 for 1730, the two sources have unlensed luminosities of $L_{1500} \simeq 0.2\,\mu_5^{-1} L^{\star}_{z=6}$, adopting $L^{\star}_{z=6}$ from Bouwens et al. (2007). Even in the more conservative case ($\mu > 5$), these are the faintest spectroscopically confirmed sources at these redshifts with such a high signal to noise (Balestra et al. 2013; Bradac et al. 2012; Schenker et al. 2012).
3. *Equivalent widths and FWHM of the lines.* The continuum is not detected in the spectra. Therefore, we derive the continuum level under the Lyα transition by using the closest *HST* band not including the line (Y105) and correcting for the UV slope β (see below). The rest-frame EWs of 859 and 1730 are 45 ± 7 Å and 32 ± 10 Å, respectively. These are typical values if compared with those observed at similar redshifts among Lyman break galaxies or Lyα emitters (Stark et al. 2011). The observed FWHM of the lines is also modest; after correcting for the instrumental profile they are $\lesssim$150 km s^{-1}.
4. *Ultraviolet spectral slope β ($F_\lambda = \lambda^\beta$).* Following Castellano et al. (2012) and Bouwens et al. (2013), ultraviolet spectral slopes were estimated by fitting the near-infrared WFC3 magnitudes redward of the Lyα line using the Y105, J125, F140W, and H160 bands (for 859 the F110W band was also available and has been included in the fit). Being achromatic, strong lensing does not affect the colors of the sources. The measured slopes for 859 and 1730 are very steep, $\beta = -3.02 \pm 0.37$ and $\beta = -3.01 \pm 0.56$. Interestingly, this similarity is again consistent with the option that these two objects are multiple images. While source 1730 is close to a bright galaxy and its photometry has to be taken with caution, source 859 is isolated and with reliable colors (Figure 2). As noted by Zackrisson et al. (2013, hereafter Z13), the possible presence of the 2175 Å dust feature may interfere with the estimate of the UV slope. However, we tend to exclude this possibility on the basis of the redshift and the Lyα emission lines that favor low dust attenuation.
5. *Size of the sources.* As reported in B13, the two sources are resolved in the *HST*/WFC3 images. Their isophotal areas (provided by SExtractor) converted into physical units are $0.8\,\mu_5^{-1}$and $0.7\,\mu_5^{-1}$ kpc^2. If they are two distinct objects, we estimate a proper separation of $\sim$30 kpc in the source plane at $z = 6.387$, for the range of models described in Section 1.
6. *Active galactic nucleus (AGN) activity.* At $z = 6.387$ the expected N v λ1240 line is not detected (see Figure 3).

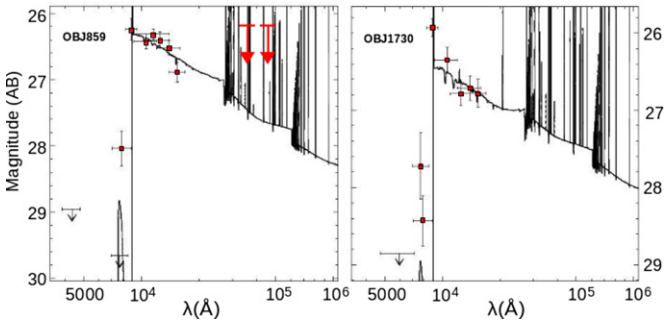

Figure 4. SED fits with the BC03 templates are shown. Nebular emission lines are included in the fit. The two arrows for 859 are 1σ lower limits of IRAC 3.6 μm and 4.5 μm channels.

(A color version of this figure is available in the online journal.)

Table 1
Observed and Physical Parameters for 859 and 1730

Quantity	macs0717_0859	macs0717_1730
R.A. (J2000)	07:17:38.18	07:17:37:85
Decl. (J2000)	+37:45:16.9	+37:44:33.7
Redshift	6.387(±0.002)	6.387(±0.003)
Y105(observed)	26.42(±0.11)	26.34(±0.16)
H160(observed)	26.88(±0.15)	26.78(±0.18)
H160(unlensed)	28.63+2.5log$_{10}(\mu_5)$	28.53+2.5log$_{10}(\mu_5)$
β_{UV}	−3.02(±0.37)	−3.01(±0.56)
SFR$_{\rm UV}(M_\odot$ yr$^{-1})$	1.6 [1–3] μ_5^{-1}	2 [1–5] μ_5^{-1}
SFR$_{\rm Ly\alpha}(M_\odot$ yr$^{-1})$	1.2 [1.0–1.4]μ_5^{-1}	1 [0.8–1.2] μ_5^{-1}
$M_\star(\times 10^7\ M_\odot)$	4 [2–12] μ_5^{-1}	2 [2–22] μ_5^{-1}
$E(B-V)$	0.0 [0.0–0.06]	0.0 [0.0–0.1]
Age (Myr)	25 [10–100]	10 [10–250]
Met. $(Z/Z_\odot)$	0.02	0.2
M1500	−18.63+2.5Log$_{10}(\mu_5)$	−18.70+2.5log$_{10}(\mu_5)$
$\times L^\star_{z=6}$	0.22 μ_5^{-1}	0.24 μ_5^{-1}
Area (kpc^2)	0.8 μ_5^{-1}	0.7 μ_5^{-1}
FWHM(Lyα)(km s^{-1})	100 [70–130]	140 [100–180]
EW$_{\rm rest}$(Lyα)(Å)	45 [38–53]	32 [22–42]
Flux(Lyα)$\times 10^{-18}$	2.8 [2.6–3.0] μ_5^{-1}	2.0 [1.8–2.3] μ_5^{-1}

Notes. Lyα fluxes are in units of erg s^{-1} cm^{-2}. Physical properties refer to the BC03 models with nebular emission and the associated 68% intervals (in parentheses) correspond to models with χ^2 probabilities higher than 0.68. The SFR(Lyα) has been derived adopting the Kennicutt (1998) conversion. Quantities related to Lyα do not include possible IGM absorption. $\mu_5 = 1$ corresponds to $\mu = 5$.

The 1σ upper limit N V/Lyα is <0.07 (typical value for AGNs is 10%; Alexandroff et al. 2013). Considering the above ratio, that only 5% of high redshift Lyman alpha emitters are possible AGNs (Malhotra et al. 2003), and that they are spatially resolved, we conclude the Lyα emission is due to star formation activity.

4. DISCUSSION AND CONCLUSIONS

As described above, the two discovered sources (or a single one in the case of multiple images) are the faintest galaxies at $z > 6$ ever observed with a spectroscopic redshift confirmation and well detected Lyα lines and spectral energy distributions (SEDs). The investigation of new luminosity regimes through strong-lensing magnification gives the opportunity to explore possible new physical conditions.

4.1. Nature of the Stellar Populations

We examine their rest-frame properties through SED analysis. We first derive physical parameters assuming ordinary stellar populations, i.e., by comparing the observed SED with a set of Bruzual & Charlot (2003) templates (BC03); assuming Salpeter initial mass function; metallicityies of 0.02, 0.2, and 1.0 $Z/Z_\odot$; and $E(B-V)$ spanning the range [0.0–1.0]. The current 1σ lower limits from IRAC (3.6 μm and 4.5 μm channels) for 859 are ≃26.1AB, too shallow to provide solid constraints on [O III] λ5007+Hβ and Hα nebular emissions. The other source, 1730, is contaminated by close brighter galaxies. The SED fitting with BC03 is shown in Figure 4 and includes nebular line and continuum emission following Schaerer & de Barros (2009; see M. Castellano et al. 2014, in preparation for further details). The output of this exercise is listed in Table 1. Regardless of the adopted μ, the two sources turn out to be very small ($\lesssim$1 kpc^2), with low star formation rates (SFRs $\simeq$ 1–2 $M_\odot$ yr^{-1}) and low stellar masses of $<10^8\ M_\odot$. The properties related to colors (i.e., independent of the magnification μ), such as dust attenuation, age, and metallicity, are consistent with newborn objects. Adopting the standard Kennicutt conversions (Kennicutt 1998) and correcting for the IGM attenuation of Lyα photons (e.g., >50%; Dijkstra & Jeeson-Daniel 2013), we obtain SFR(Lyα) $\gtrsim$ SFR(UV), where SFR(UV) is derived from the SED fit. This is indicative of ages <100 Myr, $E(B-V) \simeq 0$ (Verhamme et al. 2008), and $f_{\rm esc}$(Lyα) close to unity (Atek et al. 2008, 2014).

The SEDs can be reproduced with ordinary stellar populations, albeit the best solutions typically lie close to the edge of the parameter space (e.g., Z, age, and $E(B-V)$). Fixing $Z = Z_\odot$, the resulting ages are forced to the minimum value, 10 Myr. For this reason it is interesting to extend the investigation toward a possible presence of younger and/or extremely metal poor (EMP; $Z \simeq 1/2000\ Z_\odot$) and Pop III stars ($Z = 0$). For this purpose we consider the SED fitting and the predicted *HST*/WFC3 colors provided by Raiter et al. (2010, hereafter R10), Inoue (2011, hereafter I11), and Z13, which also include nebular contribution. The observed UV slope is compatible with either very young, but still standard (Pop II) stellar populations (BC03), or with EMP/Pop III stars. In particular, 859 (with the most reliable photometry) has a $\beta = -3.02 \pm 0.37$ that is consistent with an age $\simeq$ 1 Myr if Log$_{10}(Z/Z_\odot) = 0$ or an age $\simeq$ 1–100 Myr if Log$_{10}(Z/Z_\odot) < -4$ (as shown in I11, Figure 11).[16] Similarly, compared with the models of Z13, the UV slope is compatible with metal poor stars if ages are >10 Myr, and even Pop III if compared with R10 (assuming we are observing the stellar component). Conversely, the observed Lyα EWs would suggests that we are dealing with standard stellar populations, given that Pop III stars are often associated with Lyα $EW \sim$ 500–1500 Å rest-frame (Schaerer 2003; R10; I11). A large IGM attenuation of the Lyα line (>90%) could hide an intrinsic EW > 500 Å, making it still compatible with the Pop III interpretation. However, the influence of the IGM is highly uncertain here (see also Laursen et al. 2011; Dayal et al. 2011; Dijkstra & Jeeson-Daniel 2013). Another possibility is that the Lyα EW could be lowered for extremely metal poor ($Z/Z_\odot < 10^{-4}$) and even Pop III ($Z/Z_\odot = 0$) galaxies if $f_{\rm esc} > 0$ (Z13). For example, I11 found a Lyα EW of ≃65 Å for $Z = 0$ and 10Myr constant star formation, when $f_{\rm esc} = 0.9$.

While it is hard to make definitive statements about the populations content of these $z \sim 6.5$ sub-luminous galaxies given the current information we have about them, we observe that they are overall less evolved than their more massive counterparts and their very blue UV colors could be explained even without having to invoke Pop III stars, although we certainly cannot exclude their presence in stellar populations (e.g., Finkelstein et al. 2010). These kind of galaxies could be examples of very low chemical enrichment, dust-free systems, barely higher than the pristine gas that is probably still feeding their activity of star formation.

4.2. Cosmic Reionization

Regardless of the nature of the stellar populations, the potential role these sources have in the framework of cosmic reionization is intriguing. It is believed that the abundant, fainter

[16] We note that the probability of observing a galaxy of a few Myr old is generally small, because of its young age.

galaxies ($M_\star < 10^9\ M_\odot$) could significantly contribute to, or even be the dominant populations in, providing the ionizing radiation (e.g., Fontanot et al. 2013; Ferrara & Loeb 2013; Yajima et al. 2011; Razoumov & Sommer-Larsen 2010; but see Gnedin et al. 2008).

The direct measure of the escape fraction of ionizing radiation ($f_{\rm esc}$) is in principle possible at $z < 4$. At higher redshifts the measurement is unfeasible due to the complete IGM attenuation of the Lyman continuum. Nonetheless, it is worthwhile to investigate each of the main components that build the $f_{\rm esc}$ quantity. As discussed in Vanzella et al. (2012), the $f_{\rm esc}$ parameter is the product of the gas transmission $T_{900}^{\rm H\,I} = \exp(-\tau_{900})$ and the dust transmission $T_{\rm dust} = 10^{-0.4\times A900}$. To first order, Lyman continuum emitters should have both low dust content $A900$ and low optical depth τ_{900}. Interestingly, the two sources described in this Letter could match such requirements. First, given the very steep UV continuum the term related to dust attenuation is significantly higher than zero ($T_{\rm dust} = 10^{-0.4\times A900} \simeq 1$, as reported in Siana et al. 2007 by extrapolating the Calzetti extinction law down to the Lyman continuum, $A1500 = A900 = 0$ if $E(B-V) = 0$). Second, even though addressing the gas attenuation in the interstellar medium with current data is admittedly less reliable, it is worth noting that the presence of Lyα emission would not be in contrast with an $f_{\rm esc} > 0$. As discussed in Nakajima & Ouchi (2013), the EW(Lyα) remains almost unchanged if $f_{\rm esc}$ is $\simeq 0-0.8$. If the IGM is attenuating <70% of the line (Dijkstra & Jeeson-Daniel 2013), the resulting intrinsic FWHM ($\lesssim$300 km s^{-1}) would be in line with possible low H I column density in front of the stars (Schaerer et al. 2011). The reason is that Lyα resonance scattering is less effective if $N_{\rm H\,I}$ is low, and photons escape easily along the shorter path, decreasing the FWHM. Moreover, the observed UV slope $\beta \simeq -3$ could also indicate a deficit of nebular continuum, allowing the stellar component to emerge in the observed SED (i.e., $f_{\rm esc} > 0.5$, R10, I11, Z13). This, could, in turn, be a telltale sign of efficient feedback in these systems, capable of either sweeping away or ionizing a significant fraction of the gas surrounding the stars, a mechanism advocated by theoretical models in low-mass halos to self-regulate star formation. As a consequence, a proportionally higher fraction of ionizing radiation could be leaking out of these systems ($f_{\rm esc} > 0$) compared to their more massive counterparts and be available to keep the IGM ionized.

Regarding the single or multiple nature of the sources, the similarity in the physical and observed characteristics we derived in this work would support that they are multiple images of a single background $z = 6.4$ galaxy, but the different mass models we examined remain inconclusive regarding this option.

As discussed in Zackrisson et al. (2012) and Z13, such galaxies represent the ideal candidates for future near- and mid-infrared spectroscopic observations, especially in the investigation of the interplay between the UV slopes and the equivalent width of Hβ lines, and its relation to the $f_{\rm esc}$ parameter. Future facilities such as *JWST* and extremely large telescopes will address this issues.

We acknowledge the support from the LBT-Italian Coordination Facility for the execution of observations, data distribution, and reduction. We thank Gianni Zamorani, Marco Mignoli, and Francesco Calura for useful discussions. This work utilizes gravitational lensing models produced by PIs Bradac, Ebeling, Zitrin & Merten, Sharon, and Williams funded as part of the *HST* Frontier Fields program conducted by STScI. STScI is operated by the Association of Universities for Research in Astronomy, Inc. under NASA contract NAS 5-26555. The lens models were obtained from the Mikulski Archive for Space Telescopes (MAST). Support for A.Z. is provided by NASA through Hubble Fellowship grant #HST-HF-51334.01-A awarded by STScI. A.F. acknowledges the contribution of the EC FP7 SPACE project ASTRODEEP (Ref. No: 312725). L.I. is partially supported by CATA-Basal, Conicyt. We acknowledge financial contribution from PRIN-INAF-2010 and PRIN-INAF-2012.

REFERENCES

Alexandroff, R., Strauss, M. A., Greene, J. E., et al. 2013, MNRAS, 435, 3306
Atek, H., Kunth, D., Hayes, M., Ostlin, G., & Mas-Hesse, J. M. 2008, A&A, 488, 491
Atek, H., Kunth, D., Schaerer, D., et al. 2014, A&A, 561, A89
Balestra, I., Vanzella, E., Rosati, P., et al. 2013, A&A, 559, 9
Bouwens, R. J., Illingworth, G. D., Franx, M., & Ford, H. 2007, ApJ, 670, 928
Bouwens, R. J., Illingworth, G. D., Oesch, P. A., et al. 2013, ApJ, in press (arXiv:1306.2950)
Bradac, M., Vanzella, E., Hall, N., et al. 2012, ApJ, 755, 7
Bradley, L. D., Zitrin, A., Coe, D., et al. 2013, ApJ, in press (arXiv:1308.1692)
Bruzual, G., & Charlot, S. 2003, MNRAS, 344, 1000
Castellano, M., Fontana, A., Grazian, A., et al. 2012, A&A, 540, 39
Dayal, P., Maselli, A., & Ferrara, A. 2011, MNRAS, 410, 830
Dijkstra, M., & Jeeson-Daniel, A. 2013, MNRAS, 435, 3333
Ebeling, H., Barrett, E., Donovan, D., et al. 2007, ApJ, 661, 33
Ferrara, A., & Loeb, A. 2013, MNRAS, 431, 2826
Finkelstein, S. L., Papovich, C., Giavalisco, M., et al. 2010, ApJ, 719, 1250
Fontanot, F., Cristiani, S., Pfrommer, C., Cupani, G., & Vanzella, E. 2013, MNRAS, in press (arXiv:1312.0615)
Gnedin, N. Y., Kravtsov, A. V., & Chen, H.-W. 2008, ApJ, 672, 765
Inoue, A. K. 2011, MNRAS, 415, 2920
Kennicutt, R. C., Jr. 1998, ARA&A, 36, 189
Laursen, P., Sommer-Larsen, J., & Razoumov, A. O. 2011, ApJ, 728, 52
Limousin, M., Ebeling, H., Richard, J., et al. 2012, A&A, 544, 71
Malhotra, S., Wang, J. X., Rhoads, J. E., Heckman, T. M., & Norman, C. A. 2003, ApJ, 585, 25
Medezinski, E., Umetsu, K., Nonino, M., et al. 2013, ApJ, 777, 43
Nakajima, K., & Ouchi, M. 2013, MNRAS, in press (arXiv:1309.0207)
Postman, M., Coe, D., Benítez, N., et al. 2012, ApJS, 199, 25
Raiter, A., Schaerer, D., & Fosbury, R. A. E. 2010, A&A, 523, 64
Razoumov, A. O., & Sommer-Larsen, J. 2010, ApJ, 710, 1239
Robertson, B. E., Ellis, R. S., Dunlop, J. S., McLure, R. J., & Stark, D. P. 2010, Natur, 468, 49
Schaerer, D. 2003, A&A, 397, 527
Schaerer, D., & de Barros, S. 2009, A&A, 502, 423
Schaerer, D., Hayes, M., Verhamme, A., & Teyssier, R. 2011, A&A, 531, 12
Schenker, M. A., Stark, D. P., Ellis, R. S., et al. 2012, ApJ, 744, 179
Scodeggio, M., Franzetti, P., Garilli, B., et al. 2005, PASP, 117, 1284
Siana, B., Teplitz, H. I., Colbert, J., et al. 2007, ApJ, 668, 62
Stark, D. P., Ellis, R. S., & Ouchi, M. 2011, ApJ, 728, 2
Vanzella, E., Giavalisco, M., Dickinson, M., et al. 2009, ApJ, 695, 1163
Vanzella, E., Guo, Y., Giavalisco, M., et al. 2012, ApJ, 751, 70
Vanzella, E., Pentericci, L., Fontana, A., et al. 2011, ApJ, 730, 35
Verhamme, A., Schaerer, D., Atek, H., & Tapken, C. 2008, A&A, 491, 89
Yajima, H., Choi, J.-H., & Nagamine, K. 2011, MNRAS, 412, 411
Zackrisson, E., Inoue, A. K., & Jensen, H. 2013, ApJ, 777, 39
Zackrisson, E., Zitrin, A., Trenti, M., et al. 2012, MNRAS, 427, 2212
Zitrin, A., Broadhurst, T., Rephaeli, Y., & Sadeh, S. 2009, ApJ, 707, 102